Construction of iron and oxygen co-doped nickel phosphide based on MOF derivatives for highly efficient and long-enduring water splitting

Can Lin[a], Dingqian Wang[b], Huihui Jin[a], Pengyan Wang[a], Ding Chen[a], Bingshuai Liu[a], Shichun Mu[a,*]

[a]*State Key Laboratory of Advanced Technology for Materials Synthesis and Processing, Wuhan University of Technology, Wuhan 430070, China*

[b]*College of Polymer Science and Engineering, Sichuan University, Chengdu 610065, China*

**Corresponding author: E-mail: msc@whut.edu.cn*

Materials: Materials: Nickel nitrate hexahydrate ($Ni(NO_3)_2·6H_2O$), iron (III) nitrate nonahydrate ($Fe(NO_3)_3·9H_2O$, Aladdin), ammonium fluoride (NH_4F, Aladdin), urea ($CO(NH_2)_2$, Aladdin), N,N-Dimethylformamide (DMF, Aladdin), p–benzenedicarboxylic acid ($C_8H_4O_4$, Aladdin), sodium hypophosphite ($NaH_2PO_2·H_2O$, Aladdin), ethanol (Aladdin), Nafion (Sigma-Aldrich), IrO_2 (Sigma-Aldrich), Pt/C (20 wt%, Sigma-Aldrich). The purchased raw materials were used directly for the experiment.

Preparation of precursor ($Fe_{0.1}$-$Ni_{0.9}$-MOF/NF): Precursor $Fe_{0.1}$-$Ni_{0.9}$-MOF/NF was prepared according to previous work with minor modifications.[1] First step, $Ni(NO_3)_2·6H_2O$ (1.178 g), $Fe(NO_3)_3·9H_2O$ (0.181 g), $CO(NH_2)_2$ (1.2 g) and NH_4F (0.296 g) were dissolved in 80 mL of deionized water. The nickel foam (3 cm × 3.7 cm) washed with ethanol was transferred to the hydrothermal kettle with the solution and incubated at 120 ℃ for 6 h. The template (NiFe-LDH/NF) used for the subsequent reaction was dried under vacuum. The second step, 3.5 mmol of $C_8H_4O_4$, $Ni(NO_3)_2·6H_2O$ and $Fe(NO_3)_3·9H_2O$ were uniformly dispersed in 70 mL of DMF (the total amount of the metal salt was 5.25 mmol, wherein the ratio of the nickel salt to the iron salt was 9 to 1). Then, 5 mL of ethanol and 5 mL of H_2O were added dropwise. Stirring was continued for 30 min. The resulting solution and template (NiFe-LDH/NF) were transferred to a hydrothermal kettle at 120 ℃ for 12 h, and finally obtained $Fe_{0.1}$-$Ni_{0.9}$-MOF/NF. The precursors synthesized with different ratios of iron to nickel (0:1, 1:9, 2:8) were named FNM/NF-0, FNM/NF-1 and FNM/NF-2, respectively.

Preparation of $(Fe_{0.1}Ni_{0.9})_2P(O)$/NF: $NaH_2PO_2·H_2O$ (1 g) was placed upstream of the

tube furnace, and the obtained FNM/NF-1 (1.7 cm × 1.5 cm) was placed downstream. After that, a continuous flow of inert gas was maintained in the tube furnace, and the temperature was raised to 300 ℃ for 2 h at a heating rate of 3 ℃ per minute to finally obtain $(Fe_{0.1}Ni_{0.9})_2P(O)$/NF. $Ni_2P(O)$/NF and $(Fe_{0.2}Ni_{0.8})_2P(O)$/NF were obtained by the same phosphating method using the FNM/NF-0 and FNM/NF-2 precursors, respectively.

Electrochemical Measurements: OER and HER tests were performed at room temperature using an electrochemical workstation (CHI660E, Shanghai, China). The three-electrode system included a counter electrode (graphite rod), a reference electrode (saturated Hg/HgO electrode), and a working electrode ($Fe_xNi_{1-x}P(O)$/NF). Pt/C (IrO_2) ink was prepared by ultrasonication the mixture of 6 mg Pt/C (IrO_2), 185 uL isopropyl alcohol-water solution (the ratio of isopropyl alcohol to water is 9 to 1) and 15 uL 5 wt% Nafion. Then, the Pt/C (IrO_2) ink was loaded on NF to obtain a mass loading of 20 mg cm^{-2}. Convert all potentials to reversible hydrogen electrode (RHE) following the formula (E (RHE) = E (Hg/HgO) + 0.059 pH + 0.098 V). The obtained polarization curves were iR-compensated. Electrochemical impedance spectroscopy (EIS) was carried out at open circuit voltage with the frequency range of 10^{-1} Hz to 10^5 Hz. The double layer capacitance (C_{dl}) was determined by cyclic voltammetry curves measured by scan rates of 40, 60, 80, 100 and 120 mV s^{-1}. Faradaic efficiency test is to apply an appropriate voltage to the electrocatalysts in the electrolytic cell to cause them to generate hydrogen and oxygen, and collect the generated gas by the drainage method (record data every 200 s).

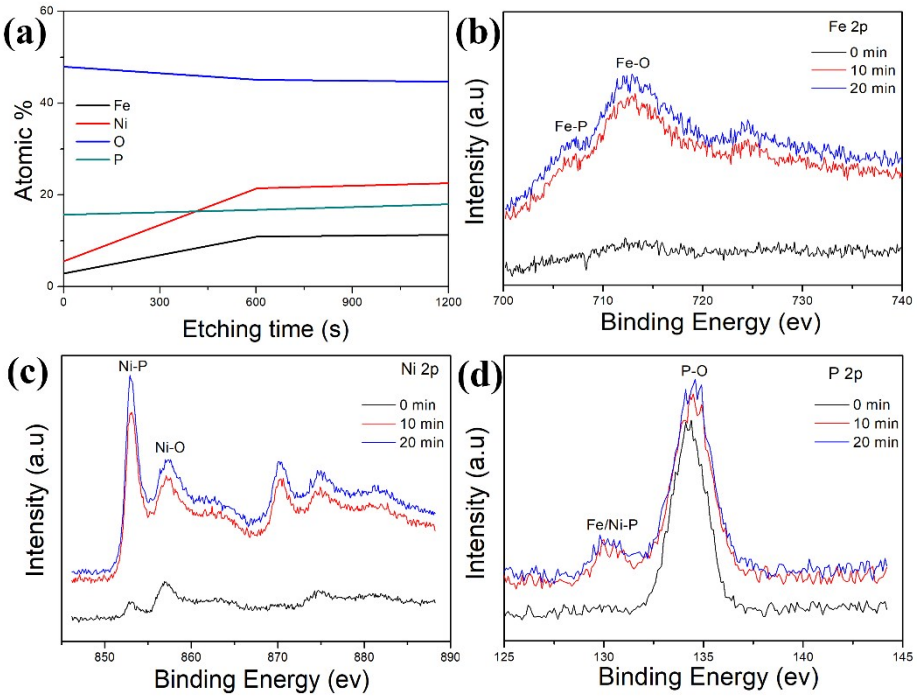

Fig. S1. (a) The atomic ratio of each element varies with Ar^+ etching time. XPS spectra in the (b) Fe 2p, (c) Ni 2p and (d) P 2p spectra for $(Fe_{0.1}Ni_{0.9})_2P(O)$/NF after 0, 10 and 20 min Ar^+ etching.

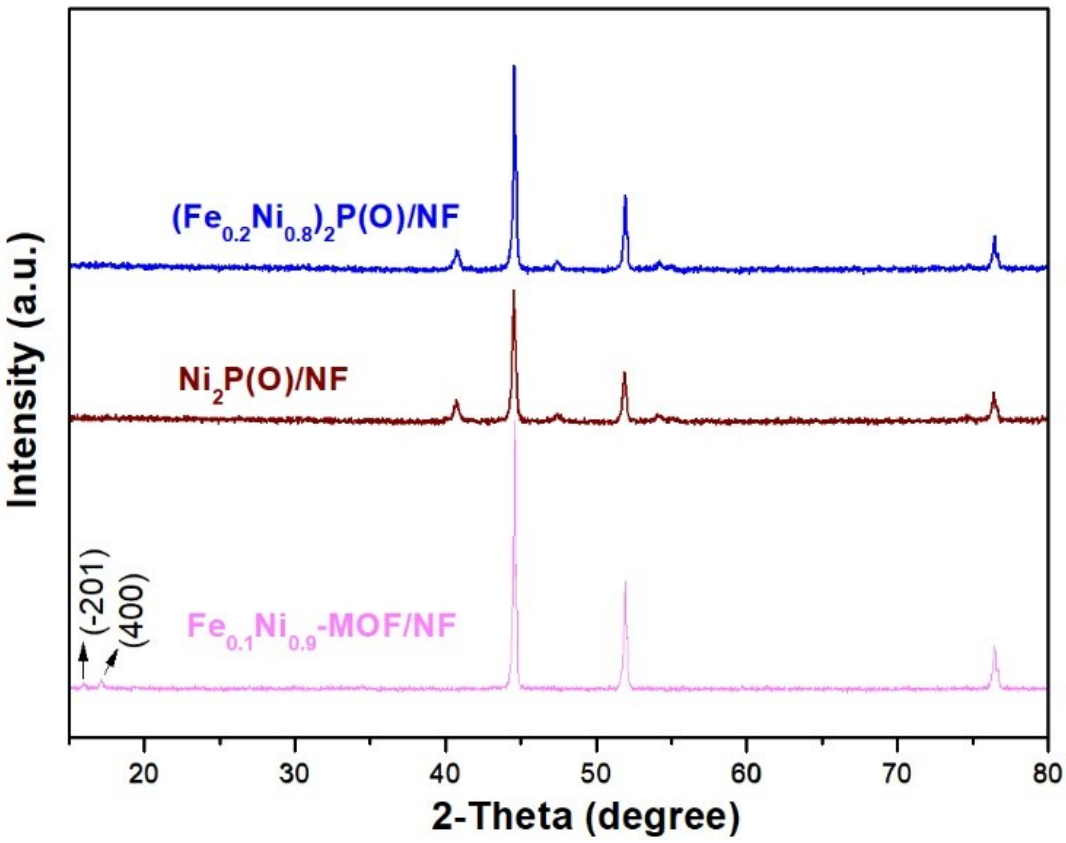

Fig. S2. XRD patterns for $Fe_{0.1}$-$Ni_{0.9}$-MOF/NF, $Ni_2P(O)$/NF and $(Fe_{0.2}Ni_{0.8})_2P(O)$/NF.

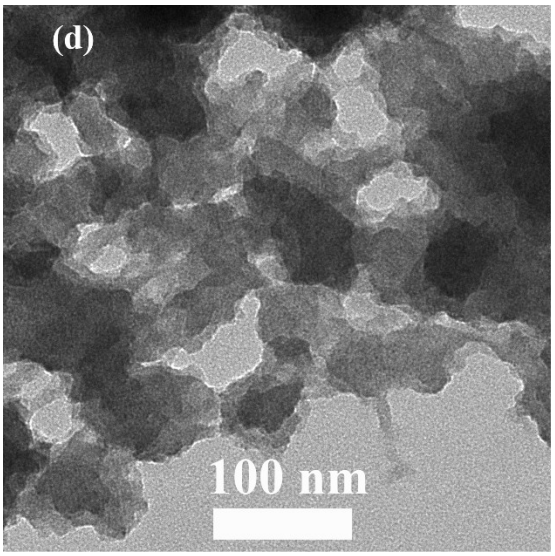

Fig. S3. TEM image of $(Fe_{0.1}Ni_{0.9})_2P(O)$/NF.

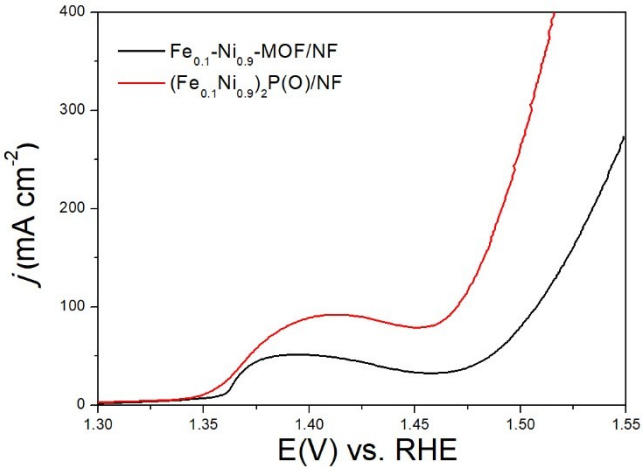

Fig. S4. OER polarization curves for $Fe_{0.1}$-$Ni_{0.9}$-MOF/NF and $(Fe_{0.1}Ni_{0.9})_2P(O)$/NF.

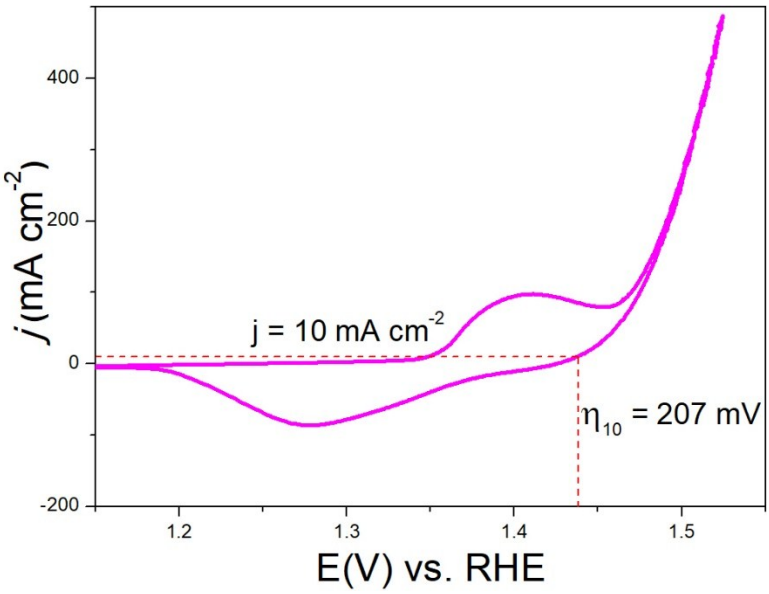

Fig. S5. Cyclic voltammogram (CV) curve recorded for $(Fe_{0.1}Ni_{0.9})_2P(O)$/NF at a sweep rate of 1 mV s^{-1} in 1.0 M KOH.

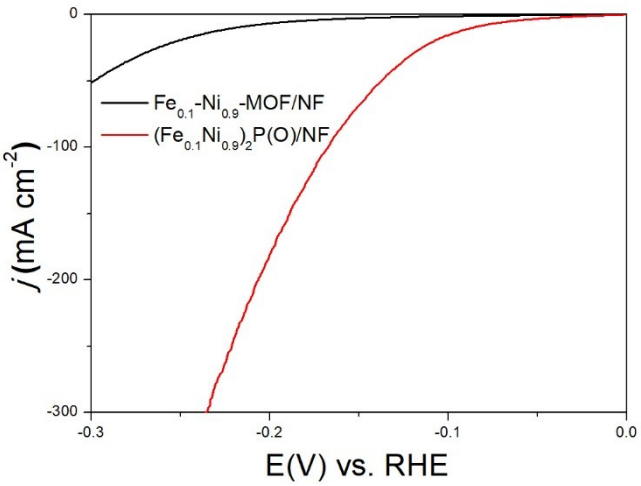

Fig. S6. HER polarization curves for $Fe_{0.1}$-$Ni_{0.9}$-MOF/NF and $(Fe_{0.1}Ni_{0.9})_2P(O)$/NF.

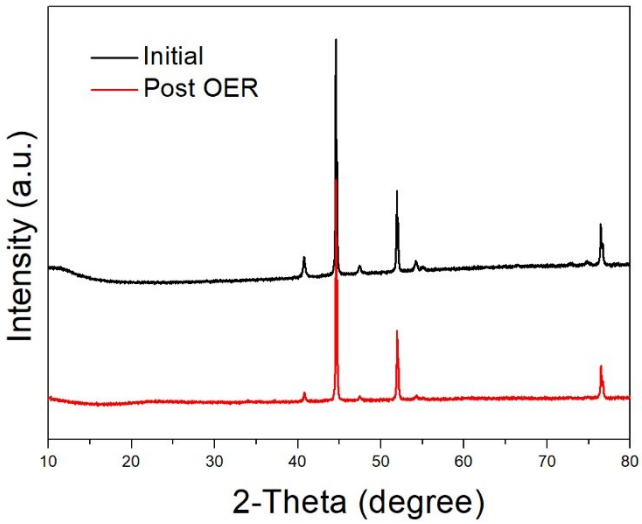

Fig. S7. XRD patterns of $(Fe_{0.1}Ni_{0.9})_2P(O)$/NF before and after OER test.

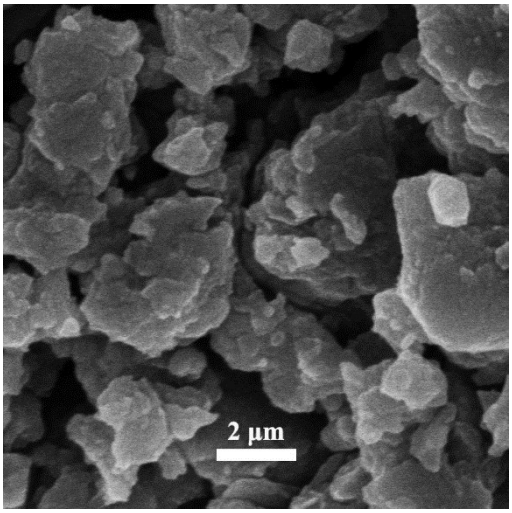

Fig. S8. The SEM image of catalyst after long-term CV stability testing of OER.

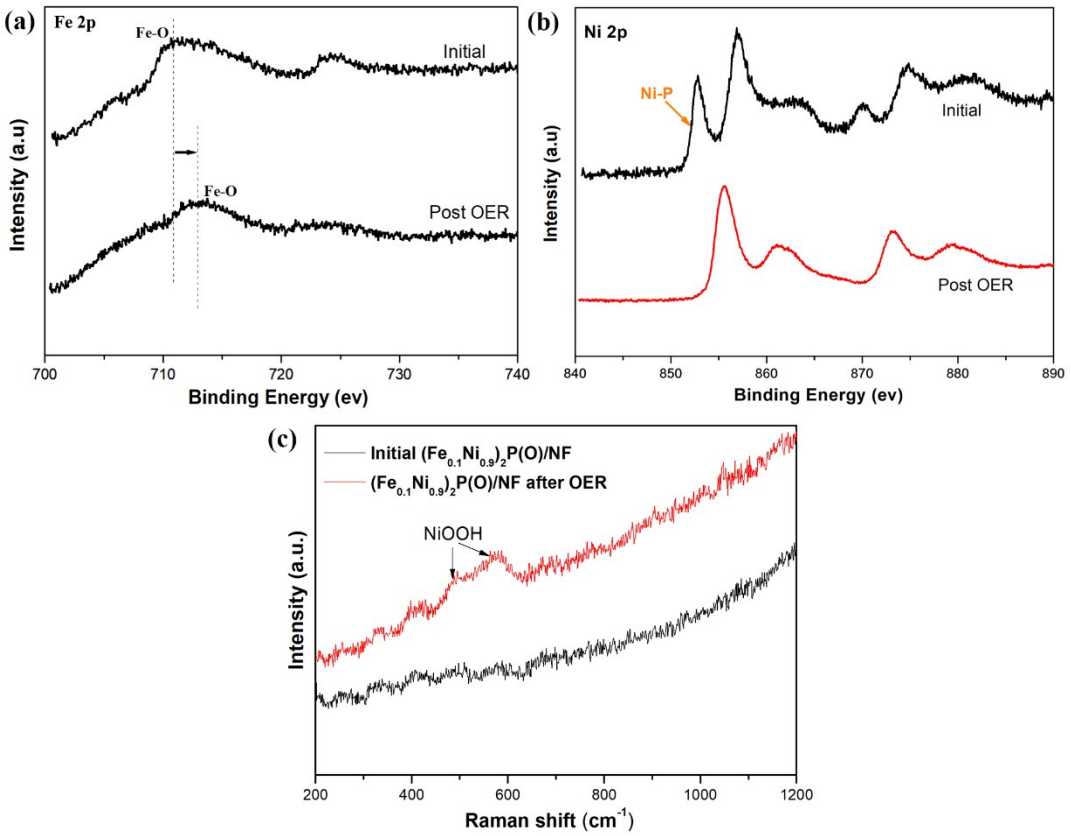

Fig. S9. XPS spectra of (a) Fe 2p and (b) Ni 2p, and (c) Raman spectra for $(Fe_{0.1}Ni_{0.9})_2P(O)/NF$ before and after OER.

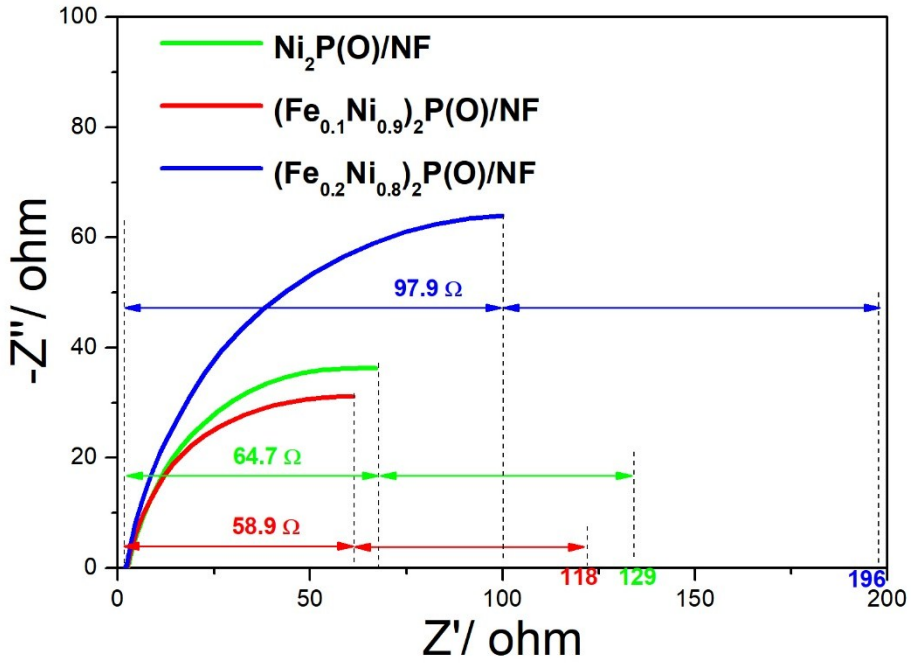

Fig. S10. EIS plots of $Ni_2P(O)/NF$, $(Fe_{0.1}Ni_{0.9})_2P(O)/NF$ and $(Fe_{0.2}Ni_{0.8})_2P(O)/NF$.

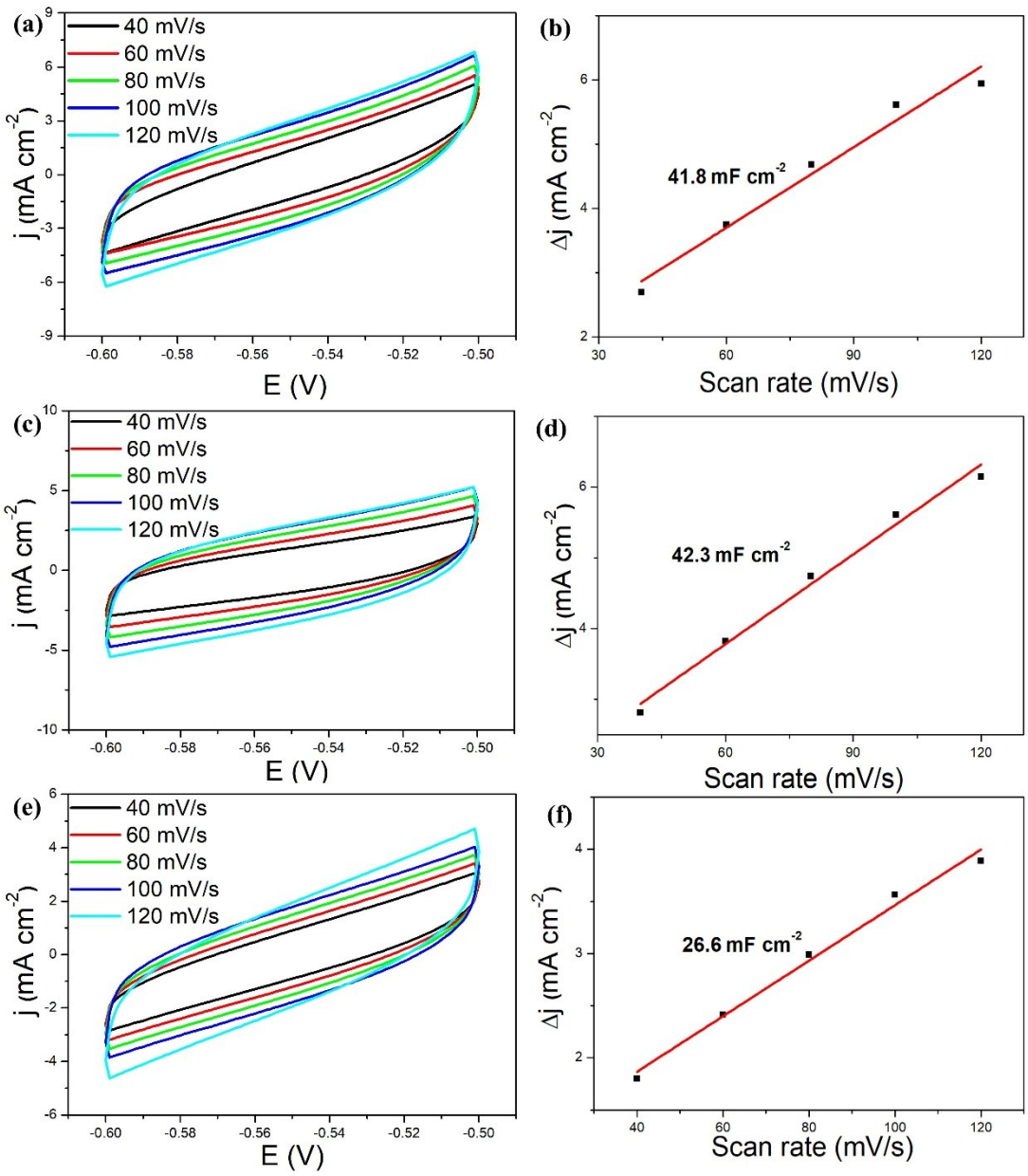

Fig. S11. CVs of (a) $Ni_2P(O)/NF$, (c) $(Fe_{0.1}Ni_{0.9})_2P(O)/NF$ and (e) $(Fe_{0.2}Ni_{0.8})_2P(O)/NF$ and corresponding current densities of (b) $Ni_2P(O)/NF$, (d) $(Fe_{0.1}Ni_{0.9})_2P(O)/NF$ and (f) $(Fe_{0.2}Ni_{0.8})_2P(O)/NF$ plotted as a function of scan rate.

Table S1. $(Fe_{0.1}Ni_{0.9})_2P(O)$/NF compared to the OER performance of other highly active OER electrocatalysts.

Electrocatalysts	Overpotential@j (mV @ mA cm^{-2})	Electrolytes	Ref.
$(Fe_{0.1}Ni_{0.9})_2P(O)$/NF	240@100	1 M KOH	This work
$(Fe_{0.1}Ni_{0.9})_2P(O)$/NF	207@10	1 M KOH	This work
Ni-Co-P HNBs	270@10	1 M KOH	2
$Co_{0.68}Fe_{0.32}P$	289@10	1 M KOH	3
Co_3O_4@Ni_2P-CoP/NF	298@50	1 M KOH	4
$Ni_{1.85}Fe_{0.15}P$/NF	270@20	1 M KOH	5
Ni-Fe-P	271@10	1 M KOH	6
$W_{0.5}Co_{0.4}Fe_{0.1}$/NF	250@10	1 M KOH	7
$Fe(TCNQ)_2$/Fe	340@10	1 M KOH	8
Mn@$Co_xMn_{3-x}O_4$	246@10	1 M KOH	9
$CuCo_2S_4$	295@100	1 M KOH	10
CoO	269@10	1 M KOH	11
Ni_3S_2	283@100	1 M KOH	12
$Ni_{4.5}Fe_{4.5}S_8$/Ni_3S_2‖Ni_3Fe	264@100	1 M KOH	13
$CoFe_2O_4$	275@10	1 M KOH	14
NCNP	370@10	0.1 M KOH	15
Fe-doped β-$Ni(OH)_2$	219@10	1 M KOH	16

Table S2. $(Fe_{0.1}Ni_{0.9})_2P(O)$/NF compared to the HER performance of other highly active HER electrocatalysts.

Electrocatalysts	Overpotential@j (mV@mA cm^{-2})	Electrolytes	Ref.
$(Fe_{0.1}Ni_{0.9})_2P(O)$/NF	87@10	1 M KOH	This work
Co-NC@Mo_2C	99@10	1 M KOH	17
$NiSe_2$-Ni_2P/NF	102@10	1 M KOH	18
$Co_{0.59}Fe_{0.41}P$	92@10	1 M KOH	19
C-WP/W	133@10	1 M KOH	20
Ni-FeP/C	95@10	1 M KOH	21
$Co_5Mo_{1.0}P$@NF	173@10	1 M KOH	22
Al-Doped Ni_2P	129@10	1 M KOH	23
$MoSe_2$–$CoSe_2$	237@10	1 M KOH	24
CeO_2–Cu_3P	148@20	1 M KOH	25
ZnS@C@MoS_2	118@10	1 M KOH	26
NiCoP	105@10	1 M KOH	27
CoP_2	184@10	1 M KOH	28
Co_xP/carbon	121@10	1 M KOH	29
FeP	95@10	1 M KOH	30
(Fe-Ni)Co_x−OH/Ni_3S_2	91@100	1 M KOH	31

Table S3. $(Fe_{0.1}Ni_{0.9})_2P(O)$/NF compared to the water-splitting performance of other highly active water-splitting electrocatalysts.

Electrocatalysts	cell voltage@j (V@mA cm^{-2})	Electrolytes	Ref.
$(Fe_{0.1}Ni_{0.9})_2P(O)$/NF	1.50@10	1 M KOH	This work
MoO_2/NF	1.53@10	1 M KOH	32
IrW	1.60@10	0.1 M KOH	33
NiSe/Ni/NC	1.60@10	1 M KOH	34
CoFe@NiFe/NF	1.59@10	1 M KOH	35
Ni QD@NC@rGO	1.563@10	1 M KOH	36
$NiFeO_x$	1.51@10	1 M KOH	37
Ni_3Te_2	1.66@10	1 M KOH	38
Fe-Ni_3S_2/NF	1.54@10	1 M KOH	39
Sulfur-doped CoP	1.78@100	1 M KOH	40
NiCo/$NiCo_2S_4$@NiCo	1.55@10	1 M KOH	41
Co-Mo_2C@NC	1.83@10	0.1 M KOH	42
CoFe@NiFe/NF	1.59@10	1 M KOH	43
Ni_3S_2/VS_4	1.57@10	1 M KOH	44
$Co_{0.75}Ni_{0.25}Se$/NF	1.60@10	1 M KOH	45
NF/H-$CoMoO_4$	1.56@10	1 M KOH	46

References

1. L. Yang, G. Zhu, H. Wen, X. Guan, X. Sun, H. Feng, W. Tian, D. Zheng, X. Cheng and Y. Yao, *J. Mater. Chem. A*, 2019, **7**, 8771-8776.
2. E. Hu, Y. Feng, J. Nai, D. Zhao, Y. Hu and X. W. Lou, *Energy Environ. Sci.*, 2018, **11**, 872-880.
3. F. Li, Y. Bu, Z. Lv, J. Mahmood, G. Han, I. Ahmad, G. Kim, Q. Zhong and J. Baek, *Small*, 2017, **13**, 6.
4. M. Guo, Y. Li, L. Zhou, Q. Zheng, W. Jie, F. Xie, C. Xu and D. Lin, *Electrochim. Acta*, 2019, **298**, 525-532.
5. P. Wang, Z. Pu, Y. Li, L. Wu, Z. Tu, M. Jiang, Z. Kou, I. Arniinu and S. Mu, *ACS Appl. Mater. Interfaces*, 2017, **9**, 26001-26007.
6. C. J. Xuan, J. Wang, W. W. Xia, Z. K. Peng, Z. X. Wu, W. Lei, K. D. Xia, H. L. L. Xin, D. L. Wang and U. N. Y. Brookhaven National Laboratory, *ACS Appl. Mater. Interfaces*, 2017, **9**, 26134-26142.
7. Y. Pi, Q. Shao, P. Wang, F. Lv, S. Guo, J. Guo and X. Huang, *Angew. Chem., Int. Ed.*, 2017, **56**, 4502-4506.
8. M. Xie, X. Xiong, L. Yang, X. Shi, A. M. Asiri and X. Sun, *Chem. Commun.*, 2018, **54**, 2300-2303.
9. C. Hu, L. Zhang, Z.-J. Zhao, J. Luo, J. Shi, Z. Huang and J. Gong, *Adv. Mater.*, 2017, **29**, 1701820.
10. L. Yang, L. Xie, X. Ren, Z. Wang, Z. Liu, G. Du, A. M. Asiri, Y. Yao and X. Sun, *Chem. Commun.*, 2018, **54**, 78-81.

11. Z. Liang, Z. Huang, H. Yuan, Z. Yang, C. Zhang, Y. Xu, W. Zhang, H. Zheng and R. Cao, *Chem. Sci.*, 2018, **9**, 6961-6968.

12. H. Zhang, H. Jiang, Y. Hu, Y. Li, Q. Xu, P. Saha and C. Li, *J. Mater. Chem. A*, 2019, **7**, 7548-7552.

13. S. Qin, J. Lei, Y. Xiong, X. Xu, X. Geng and J. Wang, *Rsc Advances*, 2019, **9**, 10231-10236.

14. H. Fang, T. Huang, D. Liang, M. Qiu, Y. Sun, S. Yao, J. Yu, M. M. Dinesh, Z. Guo, Y. Xia and S. Mao, *J. Mater. Chem. A*, 2019, **7**, 7328-7332.

15. P. Ramakrishnan, J. I. Sohn, J. Sanetuntikul and J. H. Kim, *Electrochim. Acta*, 2019, **306**, 617-626.

16. T. Kou, S. Wang, J. L. Hauser, M. Chen, S. R. J. Oliver, Y. Ye, J. Guo and Y. Li, *ACS Energy Lett.*, 2019, **4**, 622-628.

17. Q. Liang, H. Jin, Z. Wang, Y. Xiong, S. Yuan, X. Zeng, D. He and S. Mu, *Nano Energy*, 2019, **57**, 746-752.

18. P. Wang, Z. Pu, W. Li, J. Zhu, C. Zhang, Y. Zhao and S. Mu, *J. Catal.*, 2019, **377**, 600-608.

19. J. H. Hao, W. S. Yang, Z. Zhang and J. L. Tang, *Nanoscale*, 2015, **7**, 11055-11062.

20. L. Wu, Z. H. Pu, Z. K. Tu, I. S. Amiinu, S. J. Liu, P. Y. Wang and S. C. Mu, *Chem. Eng. J.*, 2017, **327**, 705-712.

21. X. F. Lu, L. Yu and X. W. Lou, *Sci. Adv.*, 2019, **5**, 9.

22. Y. Zhang, Q. Shao, S. Long and X. Huang, *Nano Energy*, 2018, **45**, 448-455.

23. H. Du, L. Xia, S. Zhu, F. Qu and F. Qu, *Chem. Commun.*, 2018, **54**, 2894-2897.

24. X. Wang, B. Zheng, B. Yu, B. Wang, W. Hou, W. Zhang and Y. Chen, *J. Mater. Chem. A*, 2018, **6**, 7842-7850.

25. Z. Wang, H. Du, Z. Liu, H. Wang, A. M. Asiri and X. Sun, *Nanoscale*, 2018, **10**, 2213-2217.

26. S. Liu, S. Li, K. Sekar, R. Li, Y. Zhu, R. Xing, K. Nakata and A. Fujishima, *Int. J. Hydrogen Energy*, 2019, **44**, 25310-25318.

27. B. Ma, Z. Yang, Y. Chen and Z. Yuan, *Nano Research*, 2019, **12**, 375-380.

28. M. Wang, C.-L. Dong, Y.-C. Huang and S. Shen, *J. Catal.*, 2019, **371**, 262-269.

29. T.-S. Kim, H. J. Song, J.-C. Kim, B. Ju and D.-W. Kim, *Small*, 2018, **14**.

30. X. Zhao, Z. Zhang, X. Cao, J. Hu, X. Wu, A. Y. R. Ng, G.-P. Lu and Z. Chen, *Appl. Catal., B*, 2020, **260**, 118156.

31. Q. Che, Q. Li, X. Chen, Y. Tan and X. Xu, *Appl. Catal., B*, 2020, **263**, 118338.

32. Y. Jin, H. Wang, J. Li, X. Yue, Y. Han, P. K. Shen and Y. Cui, *Adv. Mater.*, 2016, **28**, 3785-3790.

33. L. Fu, X. Hu, Y. Li, G. Cheng and W. Luo, *Nanoscale*, 2019, **11**, 8898-8905.

34. J. Ding, P. Wang, S. Ji, H. Wang, D. J. L. Brett and R. Wang, *Electrochim. Acta*, 2019, **300**, 93-101.

35. R. Yang, Y. Zhou, Y. Xing, D. Li, D. Jiang, M. Chen, W. Shi and S. Yuan, *Appl. Catal., B*, 2019, **253**, 131-139.

36. Z. Chen, H. Xu, Y. Ha, X. Li, M. Liu and R. Wu, *Appl. Catal., B*, 2019, **250**, 213-223.

37. H. Wang, H.-W. Lee, Y. Deng, Z. Lu, P.-C. Hsu, Y. Liu, D. Lin and Y. Cui, *Nat. Commun.*, 2015, **6**, 7261.

38. U. De Silva, J. Masud, N. Zhang, Y. Hong, W. P. R. Liyanage, M. Asle Zaeem and M. Nath, *J. Mater. Chem. A*, 2018, **6**, 7608-7622.

39. G. Zhang, Y.-S. Feng, W.-T. Lu, D. He, C.-Y. Wang, Y.-K. Li, X.-Y. Wang and F.-F. Cao, *ACS Catal.*, 2018, **8**, 5431-5441.

40. M. A. R. Anjum, M. S. Okyay, M. Kim, M. H. Lee, N. Park and J. S. Lee, *Nano Energy*, 2018, **53**, 286-295.

41. Y. Ning, D. Ma, Y. Shen, F. Wang and X. Zhang, *Electrochim. Acta*, 2018, **265**, 19-31.

42. M. Wang, S. Dipazir, P. Lu, Y. Wang, M. Yuan, S. Li and G. Zhang, *J. Colloid Interface Sci.*, 2018, **532**, 774-781.

43. R. Yang, Y. Zhou, Y. Xing, D. Li, D. Jiang, M. Chen, W. Shi and S. Yuan, *Appl. Catal., B*, 2019, **253**, 131-139.

44. D. Yang, L. Cao, L. Feng, J. Huang, K. Kajiyoshi, Y. Feng, Q. Liu, W. Li, L. Feng and G. Hai, *Appl. Catal., B*, 2019, **257**, 117911.

45. S. Liu, Y. Jiang, M. Yang, M. Zhang, Q. Guo, W. Shen, R. He and M. Li, *Nanoscale*, 2019, **11**, 7959-7966.

46. K. Chi, X. Tian, Q. Wang, Z. Zhang, X. Zhang, Y. Zhang, F. Jing, Q. Lv, W. Yao, F. Xiao and S. Wang, *J. Catal.*, 2020, **381**, 44-52.

Video S1. The water-splitting process of the electrolyzer assembled from $(Fe_{0.1}Ni_{0.9})_2P(O)$/NF.